2016 16th International Conference on Control, Automation and Systems (ICCAS 2016)
Oct. 16-19, 2016 in HICO, Gyeongju, Korea

Mechanism and Neural Network Based on PID Control of Quadcopter

Gil-Young Yoon[1*], Akito Yamamoto[2], and Hun-Ok Lim[3]

[1] Department of mechanical Engineering, Kanagawa University,
Yokohama, 220802, Japan (r201570097mb@jindai.ne.jp) * Corresponding author, Presenting author
[2] Department of R&D, Fujitsu General Limited
Kawasaki, 2130013, Japan (r201470080nn@ jindai.ne.jp)
[3] Department of mechanical Engineering, Kanagawa University,
Yokohama, 220802, Japan (holim@kanagawa-u.ac.jp)

Abstract: This paper describes mechanism the quadcopter with on-board sensors. This quadcopter consists of four rotors, four straight legs, and a disk-shaped body. The body is mainly composed of a lightweight, very rigid carbon fiber reinforced polymer (CFRP) and resin composite. A 9-axis inertial measurement unit (IMU) that contains accelerometer and gyroscope and magnetometer is installed in the body to measure rotation angles and angular velocities. In addition, a robust control method based on a neural network-based PID control method capable of dealing with payload and wind disturbances is proposed. In the control method, the gains of the PID controller are adjusted in real-time. Through several hovering experiments of the quad copter, the effectiveness of the mechanism and the control method is verified.

Keywords: Unmanned Aerial Vehicles.

1. INTRODUCTION

A quadcopter called a quadrotor drone is propelled and lifted by four rotors. An advantage of the quadcopter is that control systems are simpler than single or double rotor drones. Recently, quadcopters are being developed in institutes, universities, and for use in natural disaster areas [1, 2]. We also developed a quadcopter for the purpose of carrying payloads [3]. While the quadcopter was able to hover and fly indoors, it could not cope with wind disturbances because it controlled the payload based on only the angle position sensor.

In order to steadily carry payloads outdoors, quadcopters are designed to be strong and lightweight. Moreover, robust control methods that are capable of dealing with modeling errors, the different weight of payloads, and environmental disturbances such as wind are required. In this study, we have developed a new quadcopter to improve flight stability in windy conditions. This quadcopter consists of four legs, four rotors, and a body. Its height is 260 [mm], and its weight is 4.280 [kg]. An inertial measurement unit (IMU) is installed in the body to measure rotation angles and angular velocities. We have also developed a parameter learning method to automatically adjust PID gains. The method is based on artificial neural networks.

This paper is organized as follows: section 2 describes the mechanism of the quadcopter, section 3 describes the control method, section 4 discusses the experimental tests and results, and sections 5 provides the conclusion.

2. QUADCOPTER HARDWARE

2.1 Mechanical Hardware

The prototype of the quadcopter developed in this study is shown in Fig. 1. Its specifications are also shown in Table 1. The quadcopter consists of a disk-shaped body and four straight legs. CFRP (carbon fiber reinforced polymer) and a resin composite make up the body frame to improve its strength and reduce its weight. A gimbal that is able to control the position of the camera is installed at the lower part of the body. The propellers are loaded inside the disk-shaped body to protect them in a crash. Each rotor consists of a propeller driven by a brushless motor and generates a thrust of 1700 [g].

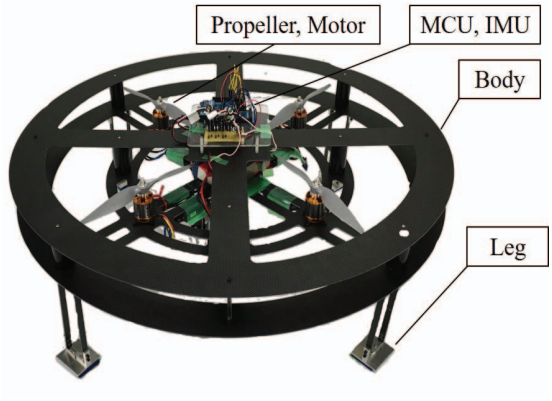

Fig. 1 Photo of quadcopter.

Table 1 Specification of quadcopter.

Height	260[mm]
Diameter	800[mm]
Weight	4280[g]
Maximum thrust	6800[g]
Propeller	10[inch]×5[pitch]

2.2 Electrical Hardware

The electrical system is shown in Fig. 2. A laptop records the position and the orientation of the quadcopter which are transmitted by radio communication. Electrical devices, such as a microcontroller board, two four-cell lithium polymer batteries (14.8[v]×2), and a sensor unit, are equipped in the center of the body. An Arduino MEGA2560 Microcontroller Revision 3 that has 54 digital input/output pins, 16 analog inputs, and 5 SPI ports is used for the control of the quadcopter. A 9-axis inertial measurement unit (IMU) that contains accelerometer and gyroscope and magnetometer is employed to

978-89-93215-12-0/16/$31.00 ⓒICROS

control the position and orientation of the quadcopter. A Wireless File Transmitter WFT-E6A and a receiver are able to control the quadcopter to fly a great distance. In addition, the XBee module that uses the ZigBee standard is employed for carrying out communication between the quadcopter and the laptop.

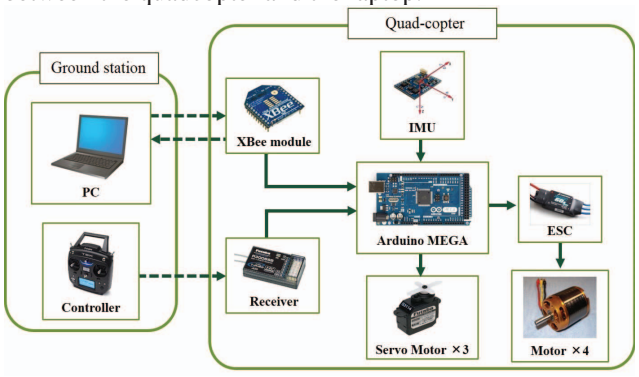

Fig. 2 Electrical system.

3. CONTROL OF QUADCOPTER

3.1 Coordinate and Modeling

To define mathematical quantities, a ground coordinate system W is arbitrarily fixed to a point on the ground, as shown in Fig. 3. X_w points to true north, Y_w points to the east, and Z_w points downward to comply with the right-hand rule. A body coordinate system B is attached at the center of gravity of the quadcopter. Furthermore, X_b points forward, Y_b is starboard, and Z_b points downward along the normal of the X_b-Y_b plane. The orientation of the quadcopter, with respect to the ground coordinate system W, is represented by Euler angles (, and)[4].

The equations of motion relative to the body frame B are calculated by using the New-Euler formulation [5]. The equations of motion are as follows:

$$\begin{cases} m\ddot{x} = (\cos\varphi\sin\theta\cos\psi + \sin\varphi\sin\psi)U \\ m\ddot{y} = (\cos\varphi\sin\theta\sin\psi - \sin\varphi\cos\psi)U \\ m\ddot{z} = mg - (\cos\varphi\cos\theta)U \\ I_x\ddot{\varphi} = \dot{\theta}\dot{\psi}(I_y - I_z) + J\dot{\theta}\Omega + T_x \\ I_y\ddot{\theta} = \dot{\varphi}\dot{\psi}(I_z - I_x) - J\dot{\varphi}\Omega + T_y \\ I_z\ddot{\psi} = \dot{\varphi}\dot{\theta}(I_x - I_y) + T_z \end{cases} \quad (1)$$

where m is the total mass and g is the acceleration due to gravity. I_x, I_y, and I_z are the moments of inertial of the quadcopter with respect to frame B. J is the moment of inertia of one propeller, Ω is a disturbance caused in the imbalance of rotor speeds. U is the lift force input, and T_x, T_y, and T_z are the roll, pitch, and yaw orientation torque inputs, respectively [6].

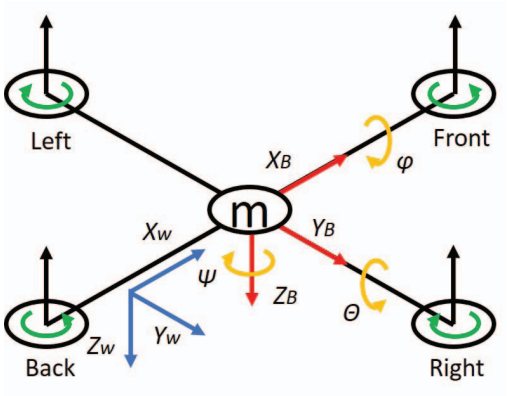

Fig. 3 Coordinate system of quadcopter.

3.2 Overview of Control System

The control system of the quadcopter is shown in Fig. 4. The quadcopter is controlled by three control methods including attitude control, altitude control, and position control. For attitude control, the errors between the target orientation angles transmitted by the controller and the orientation angles measured by the IMU are calculated in the onboard microcomputer. Moreover, the torque inputs are obtained through the PID control algorithm based on the neural network. For altitude control, the lift-force input is obtained by using the PID control, similar to the attitude control. These inputs are sent to the DC motors are controlled by Pulse Width Modulation (PWM) outputs that are calculated by the control torque, the thrust coefficients, and the drag coefficients of the propeller.

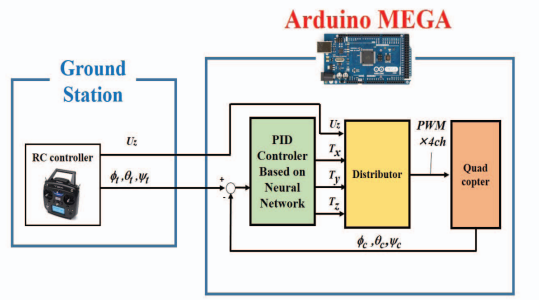

Fig. 4 Control system of quadcopter.

3.3 Neural Network Based PID Control

For mathematical modeling of the quadcopter, all dynamic effects should be considered. However, deriving an exact mathematical model is difficult because of payload and wind disturbances. In order to deal with parameter changes caused by payload disturbances, an angle sensor-based control method and an output power-adjusting method were proposed [7, 8]. However, these methods are not stable under wind disturbances.

To improve the stability of the quadrotor, we have developed a neural network-based PID control method (see Fig. 5). The gains of the PID controller are adjusted in real-time by a neural network. Fig. 6 illustrates the structure of a three-layer neural network that consists of an input layer, a hidden layer, and an output layer [9].

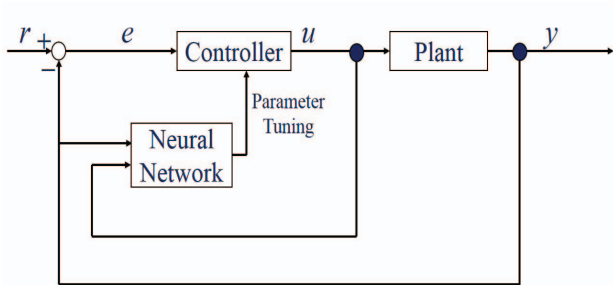

Fig. 5 Neural network based PID Control.

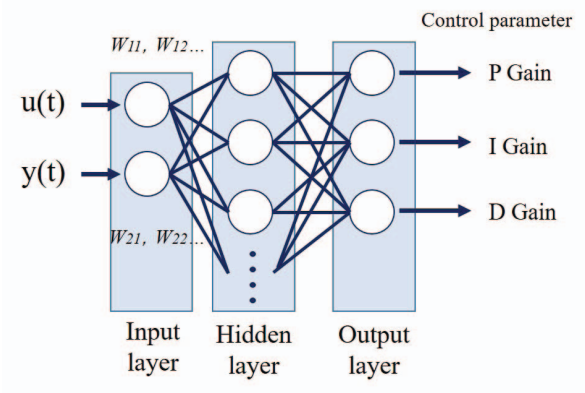

Fig. 6 Neural network structure.

The parameter inputted in each neuron is multiplied by the weight and is passed on to the adjacent neuron through a sigmoid function, as shown in Fig. 7. However, the sigmoid function is not used in the output layer.

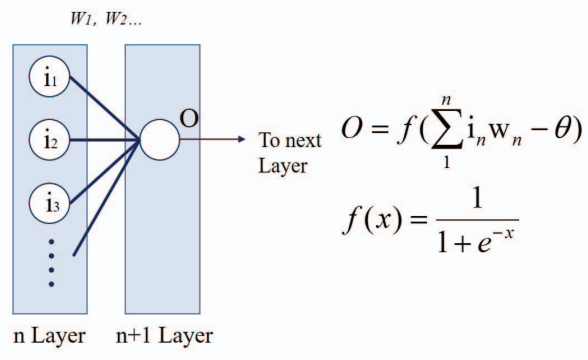

Fig. 7 Connection between two layer.

The controller gains are trained as follows. The output (O_j) if a hidden layer node j is given by:

$$O_j = f(net_j)$$
$$net_j = \sum_{i=1} W_{ji} O_i - \theta_j \quad (2)$$

where net_j is the input of a hidden layer node j. W_{ij} is the weight connecting an input layer node i and a hidden layer node j. O_i is the output of an input layer node i and θ_j is the threshold for a neuron j.

The sigmoid function is used for the activation function f.

$$f(x) = \frac{1}{1+e^{-x}}$$

The output (O_k) of an output layer node k is written by:

$$O_k = f(net_k),$$
$$net_k = \sum_{j=1} W_{kj} O_j \quad (3)$$

where net_k is the input of an output layer. W_{kj} is the weight connecting a hidden layer node j and an output layer node k.

The output O_k is employed as the gains of the PID controller. The error δ_k for the outputs of the output layer if calculated by:

$$\delta_j = e(n+1)\frac{\partial u(n)}{\partial O_j} \quad (4)$$

$$\frac{\partial un}{\partial O_k} = \begin{Bmatrix} e(n) - e(n-1)_j & k=1 \\ e(n)_j & k=2 \\ e(n) - 2e(n-1) + e(n-2)_j & k=3 \end{Bmatrix} \quad (5)$$

$$\delta_k = \sum_{k=1}^{3} \delta_k W_{kj} O_j (1 - O_j) \quad (6)$$

where $u(n)$ is the input of the quadcopter and $e(n)$ is the error.

The connection strengths between the layer nodes and the threshold value are changed by using the backpropagation algorithm [10].

$$W_{ji}(n+1) = W_{ji}(n) + \alpha \delta_j O_i \quad (7)$$
$$W_{ki}(n+1) = W_{kj}(n) + \alpha \delta_k O_j \quad (8)$$
$$\theta_j(n+1) = \theta_j(n) + \beta \delta_j \quad (9)$$

where δ_j is the error for the outputs of the hidden layer. and are the learning coefficients of the weighted value W and the threshold value θ_j respectively [11].

By repeating the above solving process, the PID gains are iteratively adjusted, and stable flight is realized. Fig. 8 shows the procedure used to learn the controller gains based on the neural network.

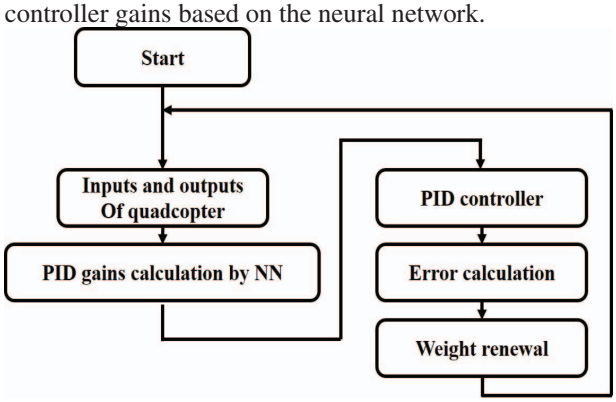

Fig. 8 Flowchart for learning controller gains by NN.

4. EXPERIMENTS AND RESULTS

4.1 Thrust force Experiment

In selecting a propeller for the quadcopter, the diameter and the pitch of the propeller should be considered. The diameter is the maximum radius of one propeller multiplied by 2, while the pitch is the distance that the propeller travels in one revolution. A propeller with a larger pitch has a higher speed. However, if the propeller`s pitch is too large, it may result in slower speed.

For measuring the propeller thrust force, an experimental system was constructed as shown in Fig. 9, was developed. A rotor was mounted on the system in reverse to generate an upward thrust force, In this study, three different size propellers were tested. When the propeller rotates, the weight is applied to the digital weight scale and the thrust force is measured.

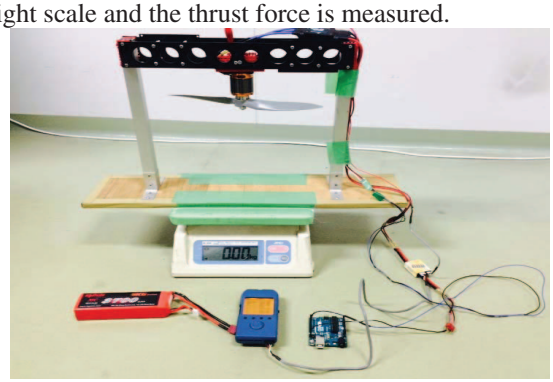

Fig. 9 Experimental system for measuring thrust force .

The thrust T is theoretically proportional to the square of the rotation speed.

$$T = C\omega^2 \qquad (10)$$

where ω is the rotational speed and C is a thrust coefficient.

Fig. 10 shows the thrust forces of three propellers. In the experiments, we can see that the 10×5 propeller can generate a higher thrust than the other propellers. Therefore, the 10×5 propeller was selected for this study.

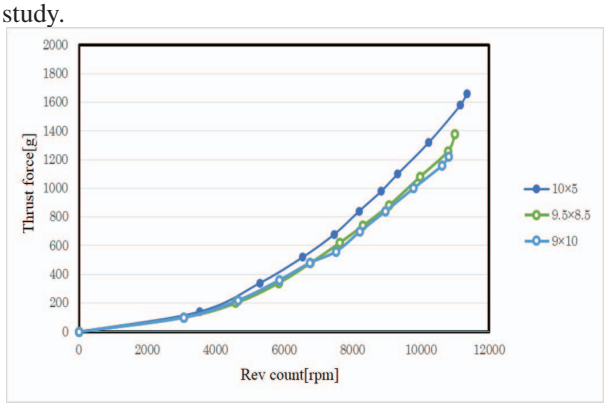

Fig. 10 Experiment results: thrust forces.

4.2 Hovering Experiment with PID Control

To confirming the effectiveness of mechanism of the quadcopter, a hovering experiment was conducted. Indoors without wind using a PID-controller. The desired angles of the roll and pitch of the quadcopter were set at 0[deg]. Fig. 11 shows the experimental results. We can see that there are ±3[deg] errors in the roll and pitch angles, respectively.

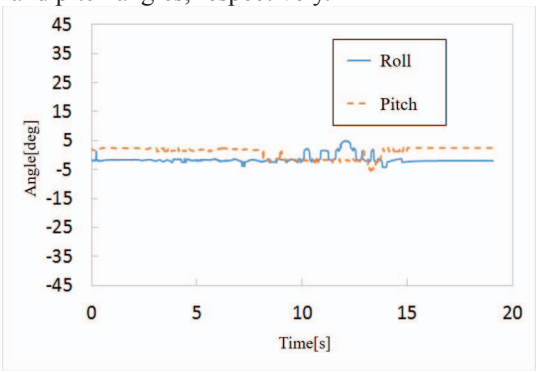

Fig. 11 Experimental result under PID control.

4.3 Hovering Experiment with Neural Network-Based PID Control

To confirm the neural network-based PID control method, hovering experiments were conducted indoors and outdoors. The weighted value W and the threshold value θj were appropriately set for the first hovering. After the first hovering, the parameter learning is repeated online by using the neural network.

Fig. 12 (a) shows the roll and pitch angles of the first experiment conducted indoors, and Fig 12 (b) shows PD gains. After the parameter learning, the roll and pitch angles and the PD gains are shown in Fig. 13 (a) and (b). The maximum errors of the roll and pitch in the first hovering are about 5 [deg] and 10 [deg]. Respectively, as shown in Fig. 12 (a). On the other hand, the maximum error of the roll and pitch after the parameter learning are about 4 [deg] and 8 [deg], respectibely, as shown in Fig. 13 (b).

The other hovering experiments were conducted outdoors with a wind speed of 4[m/s]. Fig. 14 (a) and (b) show the roll and pitch angles in the first hovering without the parameter learning and in the hovering without the parameter learning and in the hovering after the parameter learning. The maximum error of the pitch is about 25 [deg] in the first hovering. However, the maximum error of the pitch is about 10 [deg] after the learning, as shown in Fig. 14 (b).

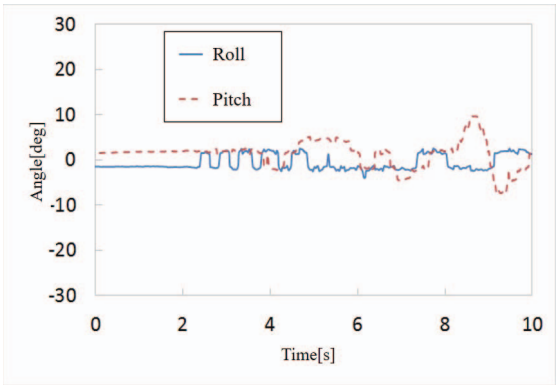

(a) Attitude angles.

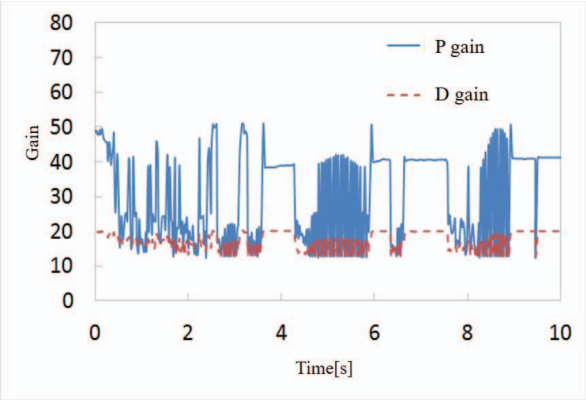

(b) PD gains.

Fig. 12 Indoor experimental results in the first hovering

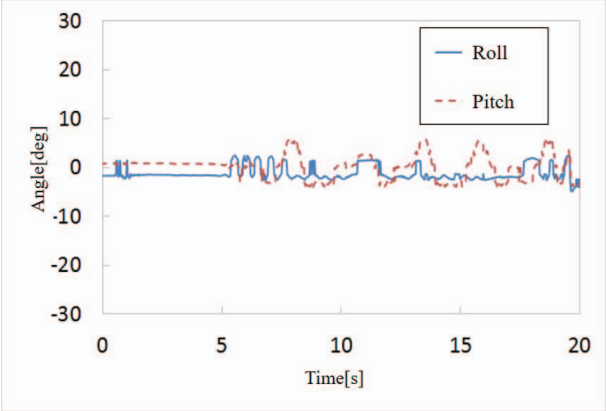

(a) Attitude angles.

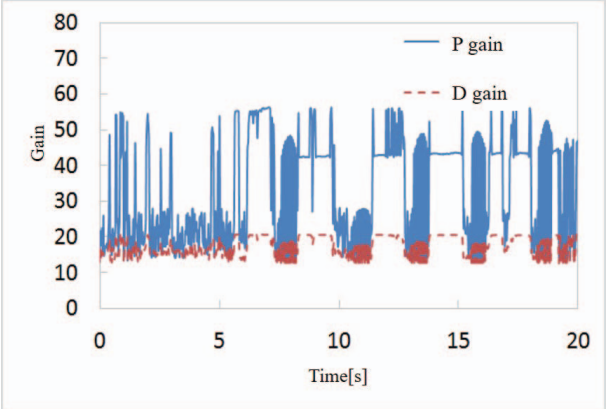

(b) PD gains.

Fig. 13 Indoor experimental results after learning.

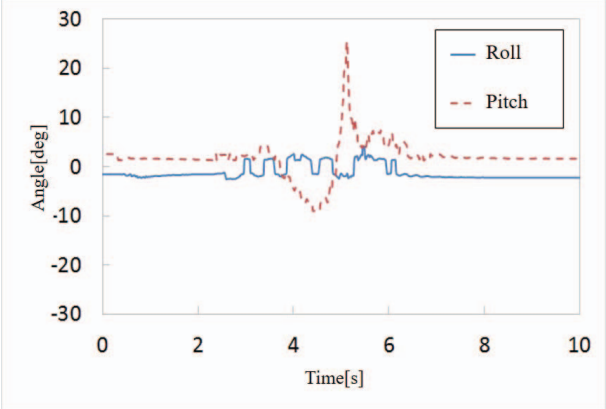

(a) Attitude angles in the first hovering.

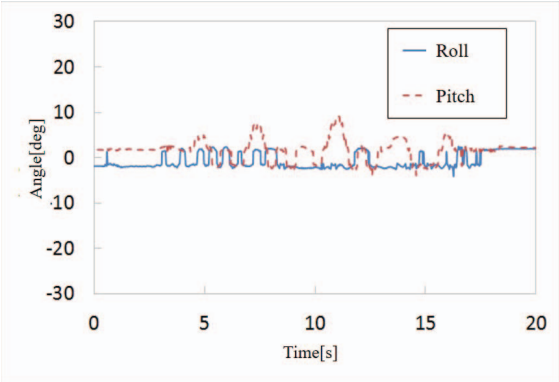

(b) Attitude angles after learning.

Fig. 14 Outdoor experimental results.

5. CONCLUSION AND FUTURE WORK

A quadcopter that is composed of a disk-shaped body and four straight legs has been developed. A gimbal capable of controlling the position of a camera was installed Moreover, neural network-based PID control method capable of dealing with parameter change caused by wind disturbances was proposed. The gains of the PID controller were adjusted in real-time. Several hovering experiments were conducted using the quadcopter, and the effectiveness of the control method was confirmed.

REFERENCES

[1] Pandit Vinay, and Poojari Arun, "A study on amazon prime air for feasibility and profitability : a Graphical Data analysis," *IOSR Journal of Business and Management,* vol. 3, pp. 6-7, 2014.

[2] E. B. Carr, "Unmanned aerial vehicles: examining the safety, security, privacy and regulatory issues of integration into U.S. airspace," *National Center for Policy Analysis*, pp. 1-39, 2013.

[3] Mizuki Sato, "A Study on control of quad-copter," *The Papers of Kanagawa Graduate school*, pp. 1– 39, 2014.

[4] O. Magnussen, and K. E. Skjonhaug, "Modeling, design and experimental study for a quad-copter system construction," University of Agder, pp. 3– 82, 2011.

[5] A. Jameson, and T. J. Baker, "Improvements to the aircraft euler method," AIAA 25th Aerospace Sciences Meeting, pp. 2-11, 1987.

[6] Teppo Luukkonen, "Modelling and control of quad-copter," *Independent Research Project in Applied Mathematics*, Espoo, pp. 3– 19, 2011.

[7] M. Habib, Pual W. Quimby, S. Chang, K. Jackson, and M. L. Commings, "Wind gust alerting for supervisory control of a micro aerial vehicle," *International Conference on IEEE Aerospace*, pp. 1– 7, 2011.

[8] A. Pyrkin, A. Bobtsov, S. Kolyubin, O. Borisov,

V. Gromov, and S. Aranovskiy, “Output Controller for quad-copters with wind disturbance cancellation,” *IEEE Multi conference on Systems and Control*, pp. 166–170, 2014.

[9] Andries P. Engelbrecht, *Computational Intelligence: An Introduction*, Wiley, 2007.

[10] F. Liao and J. Xiao, "Research on self-tuning of PID parameters based on BP Neural Networks," *Acta Simulata Systematica Sinica7*, 2005.

[11] G. Chryssoloiuris, M. Lee, and A. Ramsey, “Confidence interval prediction for neural network models,” *IEEE Transactions on Neural Networks*, Vol. 7, No. 1, pp. 229– 232, 1996.